

# Investigation of the complex dynamics and regime control in Pierce diode with the delay feedback

A.E. Hramov, and I.S. Rempen

Saratov State University, *83 Astrakhanskaja st., Saratov, 410012, Russia*

E-mail: aeh@cas.ssu.runnet.ru

KEY WORDS: Chaos, nonlinear dynamics of distributed systems, pattern formation, Pierce diode

PACS: 05.45.-a, 05.45.Gg, 05.40.-a

## Abstract

In this paper the dynamics of Pierce diode with overcritical current under the influence of delay feedback is investigated. The system without feedback demonstrates complex behaviour including chaotic regimes. The possibility of oscillation regime control depending on the delay feedback parameter values is shown. Also the paper describes construction of a finite-dimensional model of electron beam behaviour, which is based on the Galerkin approximation by linear modes expansion. The dynamics of the model is close to the one given by the distributed model.

## 1 Introduction

Pierce diode is one of the classical models of plasma microwave electronics [1–9]. This distributed model though is rather simple, demonstrates many features of the electron beam dynamics in different real electron devices. The model consists of two infinite parallel plains pierced by monoenergetic electron beam. The region between two plains is evenly filled by neutralizing stationary ions, which density is equal to the non-perturbed beam electron density. The only controlling parameter is named Pierce parameter

$$\alpha = \omega_p L / v_0,$$

where  $\omega_p$  is the electron beam plasma frequency,  $L$  is the distance between diode plains,  $v_0$  is the non-perturbed electron velocity. It was already shown that with  $\alpha > \pi$  so-named Pierce instability develops in the system and the virtual cathode is formed in the electron beam [2, 3]. At the same time in a narrow range of Pierce parameter near  $3\pi$  the increase of the instability is suppressed by the non-linearity and in the electron beam the regime without reflection realizes. In this case the system may be described by fluid equations. It was also shown that in a narrow range of Pierce parameter the system may represent chaotic dynamics [4–9].

Recently the possibilities of oscillation control in finite-dimensional dynamical systems are explored in detail [10–14]. At the same time the problem of distributed systems regime control causes great interest. For example it may be realized by adding to a system a controlled delay feedback [15, 20]. The influence of the delay feedback on the dynamics of the beam with over-critical current in the regime of virtual cathode oscillation have been already investigated and the influence of the feedback on the characteristics of generation have been shown [16]. The problem of chaos control in Pierce diode has also attracted the attention. In particular, the early work [17, 18] consider the possibility of stabilizing chaotic dynamics in Pierce diode in the regime without electrons' reflection and in the regime with virtual cathode with the help of E. Ott, C. Grebogy, J. Yorke [10] method. In our work [19] we analyse the possibility of stabilizing of chaotic dynamics of the fluid model of Pierce diode using the continuous delay feedback [11].

But the practical realization of such schemes in microwave devices come across several difficulties. So the investigation of chaotic dynamics of distributed active media with external delay feedback causes great interest.

So it seems interesting to examine the delay feedback influence on the dynamics of the system without virtual cathode – the fluid model of Pierce diode – because it represents all the classical regimes of a real distributed self-oscillation model. In this work the influence of the feedback parameters to the system characteristics is examined. The distributed chaotic system is analysed with the help of the numerical modelling of the original system of in

partial derivative non-linear equations and with the use of finite-dimensional model.

The structure of the work is the follows. In section 2 we discuss the fluid model of the Pierce diode without feedback. In section 3 explored in detail the dynamics of this model with the added delay feedback depending on the value of delay time and feedback amplitude. The finite dimensional model of the investigated system using the Galerkin method is constructed and its behavior under the influence of the delay feedback is investigated in section 4. The dynamics of finite-dimensional model is compared with the behaviour of the electron beam in the distributed system.

## 2 Explored model

The dynamics of Pierce diode processes in fluid electronics approximation is described by movement, continuity and Poisson equations:

$$\frac{\partial v}{\partial t} + v \frac{\partial v}{\partial x} = -\frac{\partial \varphi}{\partial x}, \quad (1)$$

$$\frac{\partial \rho}{\partial t} + v \frac{\partial \rho}{\partial x} + \rho \frac{\partial v}{\partial x} = 0, \quad (2)$$

$$\frac{\partial^2 \varphi}{\partial x^2} = \alpha^2(\rho - 1), \quad (3)$$

where  $\varphi$  is the space charge field potential,  $\rho$  is the electron density,  $v$  is the electron beam velocity.

The boundary conditions are:

$$v(0, t) = v_0, \quad \rho(0, t) = \rho_0, \quad \varphi(0, t) = \varphi(1, t) = 0. \quad (4)$$

The initial conditions are taken as a small perturbation of the space charge density near the homogeneous equilibrium state

$$v(x) = v_0, \quad \rho(x) = \rho_0, \quad \varphi(x) = \varphi_0$$

as  $\rho(x, 0) = \tilde{\rho} \sin 2\pi x$  where  $\tilde{\rho} \ll 1$ . The equilibrium state becomes unstable then  $\alpha > \pi$ . In the equations the normalized values are used.

The delay feedback is brought in by modelling the potential difference between entrance and exit grids by the signal taken off from the interaction space in the point  $x = x_{df}$ . As a control signal the oscillations of the space charge density  $\rho(x_{df}, t)$  is used. It can be interpreted as connecting a waveguide with a delay line to the interaction space, which is excited by the electron beam oscillations. Adding the delay feedback into the model leads to the changes in the right boundary conditions

$$\varphi(1, t) = f_{df}(t) = A(\rho(x_{df}, t - d) - \rho_0).$$

Here  $A$  is the delay feedback coefficient, characterizing the part of the oscillation power branched to the feedback delay line,  $d$  is the delay time value. Assuming that the development of the processes in our system begins at  $t = 0$  and when  $t < 0$  the space charge density is non-perturbed  $\rho(x, t) = \rho_0$ , the initial distribution of the delay feedback function is written as

$$f_{df}(t)|_{t \in [-d, 0]} = 0.$$

We have found out that the point of connection  $x_{df}$  does not influence upon the dynamics of the system. In this work value  $x_{df}$  is fixed as  $x_{df} = 0.2$ .

Numerical solution of the equations (1) and (2) is found using explicit scheme with differences against flow. Poisson equation (3) is integrated using error vector propagation (EVP) method [21].

### 3 Delay feedback influence on the nonlinear dynamics of electron beam

In Pierce diode without delay feedback when  $\alpha$  decreases from  $2.88\pi$  to  $2.86\pi$  the behaviour of the electron beam changes from regular via period doubling cascade to weakly chaotic with neatly expressed time scale. With the further decrease of Pierce parameter the chaotic oscillations of the beam complicate essentially, the time scale disappears and spectral distribution complicates. We call this two types of chaotic behaviour ribbon and spiral chaos. All

the results described in this paper have been derived for  $\alpha = 2.86\pi$ , i.e. a system without delay feedback must represent the "spiral chaos" oscillations. As quantitative characteristics of oscillation regime correlation dimension  $D$  [22] and highest Lyapunov index  $\lambda$  [23] for the restored attractor are taken. This values do not change in the different points of interaction space  $D = 2.18 \div 0.01$ ,  $\lambda = 0.16 \div 0.04$ . In figure 1 the different regimes are represented on the  $A$ - $d$  parameter plane with  $\alpha = 2.86\pi$ .

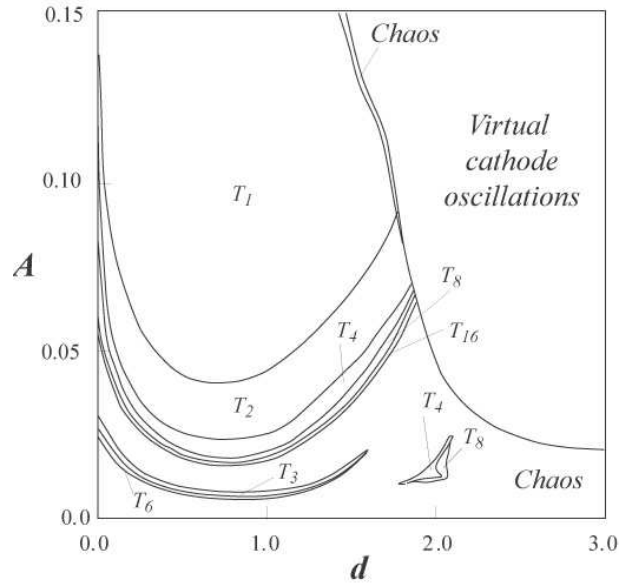


Figure 1: Oscillation regimes reproduced on parameter plane  $(A, d)$  ( $\alpha = 2.86\pi$ ,  $x_{df} = 0.2$ )

For comparison the non-dimensional characteristic time of oscillations in the electron beam  $\tau = 4.06$ . The areas of  $n$ -periodical oscillations on the parameter plane are marked as  $T_n$ . When  $A \ll 1$  the system demonstrates chaotic oscillations identical to those without feedback.

In figure 2 the phase-plane portraits, spectrums and time series for the "spiral" chaos regime (a), weakly developed chaos (b) and regular (period 1) oscillations (c) are represented. The phase-plane portraits are reconstructed by Takens delay method [24] from the time series characterizing the oscillation of the space charge density in the fixed point of the distributed system.

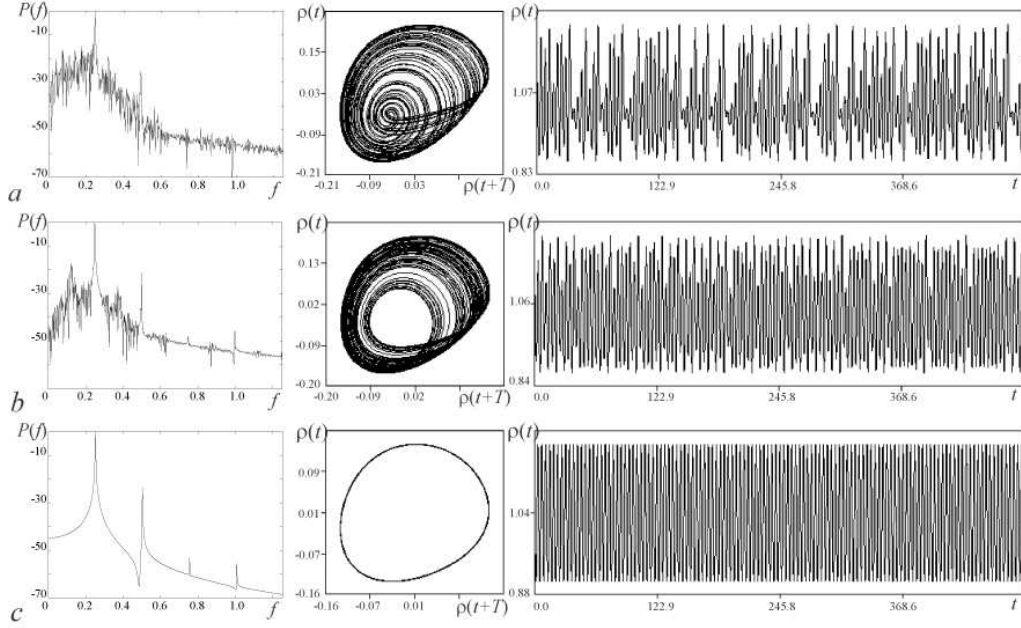


Figure 2: Phase portraits, spectrums and time series of electron beam oscillations for the cases of “spiral” chaos regime (a), weakly developed chaos (b) and regular (period 1) (c) regimes

Though system behaviour (a) is rather complex, in the frequency spectrum one can see the base frequency  $f_0 = 1/\tau = 0.25$  and its second harmony  $2f_0$ . Analyzing the system attractor in phase-plane space one can see that near the instable state  $\rho = \rho_0$  there is a loop on which the motion of the phase point become slower. The other space of attractor is tightly filled by spiral phase pathes. When  $A$  increases the behaviour of the system may be different depending on the value of delay time  $d$ . If  $d > \tau/2$  the complexity of electron beam dynamics increases with the increasing of  $A$ . The frequency spectrum and the phase-plane portrait become more complex too, the oscillation amplitude enlarges. Further enlargement of  $A$  leads to essentially different dynamics of the system. The oscillation amplitude sharply increases and then in the electron beam the reflected electrons appear. In the system appears the virtual cathode. The electron beam behaviour is determined by two mechanisms - the Pierce instability and its limitation by the nonlinearity.

The delay feedback with parameter values  $d > 1.8 \div 2$   $A > 0.02$  destroys the limitation mechanism and leads to the increasing of instability and further to virtual cathode forming. In this case the fluid model becomes incorrect because equations (1), (2) describes the processes in the electron beam only without overtaking or reflection. The threshold value  $A_{VC}$  depends on the value of  $d$ . In the case  $d < \tau/2$  the complexity of the electron beam oscillation decreases with the increase of  $A$ . The noise base diminishes, with the further enlargement of  $A$  on the bifurcation map one can see periodic gaps. When  $A > 0.03$  a transition from the chaotic to periodical dynamics via reverse doubling period cascade have place. The oscillation amplitude decreases and approach to non-perturbed value  $\rho_0$ . In a wide range of feedback parameters it is possible to suppress the chaotic dynamics of the electron beam and to establish the regular one. In figure 1 the areas of cycles 1-16 period and transitions between different regimes depending on the changes of delay feedback parameters are shown.

Now some words about the physical processes in the electron beam. As the explorations of the electron waves propagation show, dynamics of electron beam is mainly determined by the distance between the current state of the system and the homogeneous equilibrium state  $\rho(x) = \rho_0$ ,  $v(x) = v_0$ ,  $\varphi(x) = \varphi_0$ . The distance between the current state of the system and the homogeneous equilibrium state can be determined as

$$S(t) = \left( \int_0^1 (\rho(x, t) - \rho_0)^2 + (\varphi(x, t) - \varphi_0)^2 + (v(x, t) - v_0)^2 dx \right)^{1/2}. \quad (5)$$

Time-dependent changes of this value illustrates figure 3 for the cases of spiral chaos regime (a), weakly developed chaos (b) and regular (period 1) oscillations (c).

In the first case the system in some time comes very close to the homogeneous equilibrium state  $S \sim 0$  and the oscillation amplitude is very small. Then the mechanism of instability activates and the amplitude of the oscillations increases until it's limited by the nonlinearity. Then the process repeats, but each time  $S$  and the space distributions of the values near the

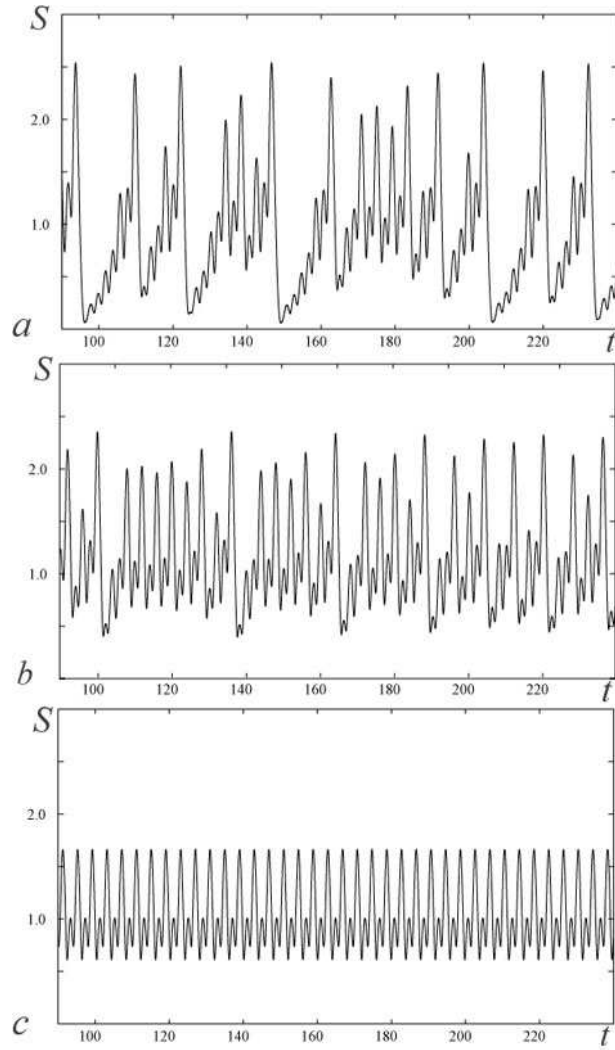


Figure 3: The distance between the current state of the system and the homogeneous equilibrium state depending on time for the cases of "spiral" chaos regime (a), weakly developed chaos (b) and regular (period 1) (c) regimes

equilibrium state are different, so the development of instability begins from another conditions and the dynamics of the system is irregular. The dynamics of the system can also be examined by considering non-linear energetic



functionals [25]:

$$W_k = \frac{1}{2} \int_0^1 \rho v^2 dx - \frac{1}{2}, \quad W_p = \frac{1}{2} \int_0^1 \rho \varphi dx \quad (6)$$

These functions describe energy transitions between kinetic energy of the beam movement and potential energy of the space charge field. One can see that for the chaotic regimes the maximums of the functionals are larger than those for the regular processes, because of the larger degree of non-linearity in the chaotic regime.

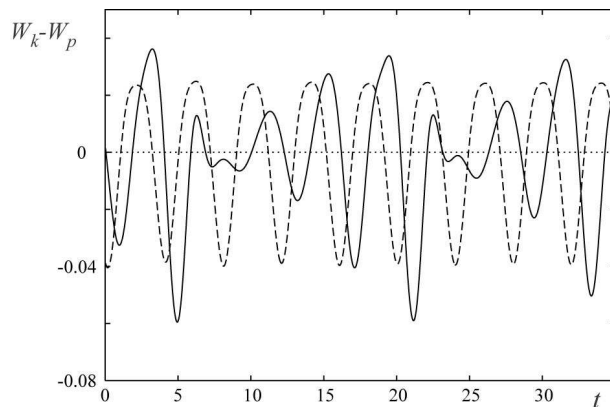


Figure 4: Difference between kinetic energy and potential energy of the beam movement  $\Delta W = W_k - W_p$  for the cases of "spiral" chaos regime (solid line) and regular regime (dotted line)

Figure 4 illustrates the time-dependence of the function  $\Delta W = W_k - W_p$  characterizing the energy transition processes in the electron beam. In the periodic regime (the dotted line) the energy transitions are regular. The maximums of the functions shows the accumulation of the charge in the interaction space. In the chaotic regime (the solid line) in some moments the energy difference  $\Delta W = 0$ . The system nears to the unstable equilibrium state. Then the wave movement energy increases again abruptly. Further the perturbation energy decreases and the system protractedly is situated near the equilibrium state. It can be physically explained as follows: in the electron beam the stationary wave of electron density appears. Its amplitude

increases abruptly near the exit grid. Then the electromagnetic field of this clot brakes the following electrons and the result is that much more electrons leave the interaction gap then enter it. The discussed values approach the equilibrium state and then the process repeats from the new starting point. The feedback destroys this mechanism. When the delay time  $d < \tau/2$  the system cannot approach the equilibrium state because the feedback signal extenuates the stored charge in the exit region and promotes the acceleration of the beam in the instant time when  $\Delta W$  is maximal. And vice versa when  $d < \tau/2$  the feedback signal leads to the increasing of oscillation amplitude, the system dynamics become more complicate and with sufficiently large  $A$  the virtual cathode appears.

## 4 Finite-dimensional model of electron beam dynamics

In [2] the method of constructing a finite-dimensional model based on the Galerkin approximation by linear modes expansion is described. It has been shown by [26] that in the range of Pierce parameter variation  $\alpha \in (2\pi, 3\pi)$  in the system excites infinite number of modes which can be determined from the dispersion equation

$$\left\{ \exp[j\alpha\varpi] [(\varpi^2 + 1) \sin \alpha + 2j\varpi \cos \alpha] + \alpha\varpi^4 - \alpha\varpi^2 - 2j\varpi \right\} (\varpi^2 - 1)^{-2} = 0, \quad (7)$$

where  $\varpi = \omega/\omega_p$ . In the case of Pierce diode system the modes were determined by Kuhn (1986). It have been shown that among the excited modes only three were damping rather slowly and containing the most part of the system energy. So for the description of the system dynamics it is enough to take into account only this three modes. For the different Pierce parameter values corresponding to different dynamical regimes the space distributions vary weakly, so we can suppose they are independent of  $\alpha$ . The initial basis

for the finite-dimensional approximation is taken as

$$\begin{aligned}
v &= \sum_{i=1}^3 V_i(x) a_i(t), \\
\rho &= \sum_{i=1}^3 R_i(x) a_i(t), \\
\varphi &= \sum_{i=1}^3 \Phi_i(x) a_i(t),
\end{aligned} \tag{8}$$

where  $R_i, V_i, \Phi_i$  are the space distributions modes for the  $\lambda_i$ ,  $\alpha_i$  are the modes amplitudes. Substituting the trial solution (8) into system (1)-(3), written for weakly perturbed values, we derive the nullity vector  $\vec{\Psi} = (\Psi_1, \Psi_2, \Psi_3)$ , which components can be written as

$$\begin{aligned}
\Psi_1 &= \dot{a}_1 R_1 + \dot{a}_2 R_2 + \dot{a}_3 R_3 + a_1(R_{1x} + V_{1x}) + \\
&\quad + a_2(R_{2x} + V_{2x}) + a_3(R_{3x} + V_{3x}) + \\
&\quad + a_1^2(R_1 V_1)_x + a_2^2(R_2 V_2)_x + a_3^2(R_3 V_3)_x + \\
&\quad + a_1 a_2(R_1 V_2 + R_2 V_1)_x + a_1 a_3(R_1 V_3 + R_3 V_1)_x + \\
&\quad + a_2 a_3(R_2 V_3 + R_3 V_2)_x,
\end{aligned} \tag{9}$$

$$\begin{aligned}
\Psi_2 &= \dot{a}_1 V_1 + \dot{a}_2 V_2 + \dot{a}_3 V_3 + a_1(\Phi_{1x} + V_{1x}) + \\
&\quad + a_2(\Phi_{2x} + V_{2x}) + a_3(\Phi_{3x} + V_{3x}) + \\
&\quad + a_1^2 V_1 V_{1x} + a_2^2 V_2 V_{2x} + a_3^2 V_3 V_{3x} + \\
&\quad + a_1 a_2(V_1 V_{2x} + V_2 V_{1x}) + a_1 a_3(V_1 V_{3x} + V_3 V_{1x}) + \\
&\quad + a_2 a_3(V_2 V_{3x} + V_3 V_{2x}),
\end{aligned} \tag{10}$$

$$\begin{aligned}
\Psi_3 &= a_1(\Phi_{1xx} + \alpha^2 R_1) + a_2(\Phi_{2xx} + \alpha^2 R_2) + \\
&\quad + a_3(\Phi_{3xx} + \alpha^2 R_3),
\end{aligned} \tag{11}$$

where  $(\cdot)_x = \frac{\partial}{\partial x}(\cdot)$ .

The internal product of functions is defined as

$$(f \times g) = \int_0^1 fg dx. \quad (12)$$

Using Galerkin method we can find the unknown coefficients  $a_i$  from the matrix equation

$$\left( \left( \begin{array}{ccc} R_1 & V_1 & \Phi_1 \\ R_2 & V_2 & \Phi_2 \\ R_3 & V_3 & \Phi_3 \end{array} \right) \times \left( \begin{array}{c} \Psi_1 \\ \Psi_2 \\ \Psi_3 \end{array} \right) \right) = 0. \quad (13)$$

Carrying out elementary transformation and taking into account the equations (9)–(11), we derive the matrix equation for the coefficients  $a_i$ :

$$\mathbf{M}\dot{\mathbf{A}} + \mathbf{B}\mathbf{A} + \mathbf{D} = 0, \quad (14)$$

where vector  $\mathbf{A}$  is composed from coefficients  $a_i$ . The elements of matrixes  $\mathbf{M}$  and  $\mathbf{B}$  are derived as

$$\begin{aligned} m_{i,j} &= (R_j \times R_i) + (V_j \times R_i), \\ b_{i,j} &= ((R_{ix} + V_{ix}) \times R_j) + ((V_{ix} + \Phi_{ix}) \times V_j) + \\ &\quad + ((\Phi_{ixx} + \alpha^2 R_i) \times \Phi_j). \end{aligned}$$

Matrix element  $\mathbf{D}$  is derived from formula

$$\begin{aligned} d_i &= \sum_k a_k^2 [(R_k V_k)_x R_i + V_k V_{kx} V_i] + \\ &\quad + \sum_k \sum_{l, l \neq k} a_k a_l [(R_k V_l + R_l V_k)_x R_i + \\ &\quad \quad + (V_k V_{lx} + V_l V_{kx}) V_i]. \end{aligned}$$

Resolving the equations (14) relatively  $\dot{a}_i$ , we derive the explicit equations:

$$\begin{aligned} \dot{a}_1(t) &= l_{11}a_1 + l_{12}a_2 + l_{13}a_3 + l_{14}a_1^2 + l_{15}a_2^2 + \\ &\quad + l_{16}a_3^2 + l_{17}a_2a_3 + l_{18}a_1a_1 + l_{19}a_1a_3, \end{aligned} \quad (15)$$

$$\begin{aligned}\dot{a}_2(t) = & l_{21}a_1 + l_{22}a_2 + l_{23}a_3 + l_{24}a_1^2 + l_{25}a_2^2 + \\ & + l_{26}a_3^2 + l_{27}a_2a_3 + l_{28}a_1a_1 + l_{29}a_1a_3,\end{aligned}\quad (16)$$

$$\begin{aligned}\dot{a}_3(t) = & l_{31}a_1 + l_{32}a_2 + l_{33}a_3 + l_{34}a_1^2 + l_{35}a_2^2 + \\ & + l_{36}a_3^2 + l_{37}a_2a_3 + l_{38}a_1a_1 + l_{39}a_1a_3.\end{aligned}\quad (17)$$

The coefficients  $l_{ij}$  are derived from numerical solution of the implicit equations and are independent of Pierce parameter variations. The non-linearities of the system are quadratic and appears because of the kinematic non-linearities and those presenting in continuity equation. The 1 and 2 modes are excited by the instability negative dissipation and its energy is inherited into the 3rd mode. As the numerical analysis shows the finite-dimensional demonstrates the same types of behaviour as the distributed one. With the decrease of  $\alpha$  the system dynamics becomes more complex and further transition to chaos via period doubling cascade takes place. The comparison of bifurcation diagrams for the distributed model and the finite-dimensional model is made in figure 5.

Also in the system two variants of the chaotic regime similar to those in the distributed model are observed – the "spiral" chaos and the "band" chaos. The delay feedback is brought in by adding into the right part of the equations (7)-(9) the signal  $F_{df}(t - d)$  which is formed as:

$$F_{df}(t) = A[a_1(t) + a_2(t) + a_3(t)] \quad (18)$$

In figure 6 the bifurcation map in the parameters  $A - d$  for the finite-dimensional model is presented. The Pierce parameter  $\alpha = 2.774\pi$ . With this parameter value in the system without feedback the "spiral" chaotic oscillations are observed. In the map we can see that with the increase of feedback signal amplitude and  $d < \tau/2$  (where  $\tau \approx 3.15 = 1/f_0$ ,  $f_0$  - the base spectrum frequency) the chaotic dynamics is suppressed and regular regime is installed.

When  $d > \tau/2$  the oscillation amplitude sharply increases which is equal to system transition to virtual cathode forming regime, where the finite-dimensional equations become incorrect. Comparing figure 1 and figure 4

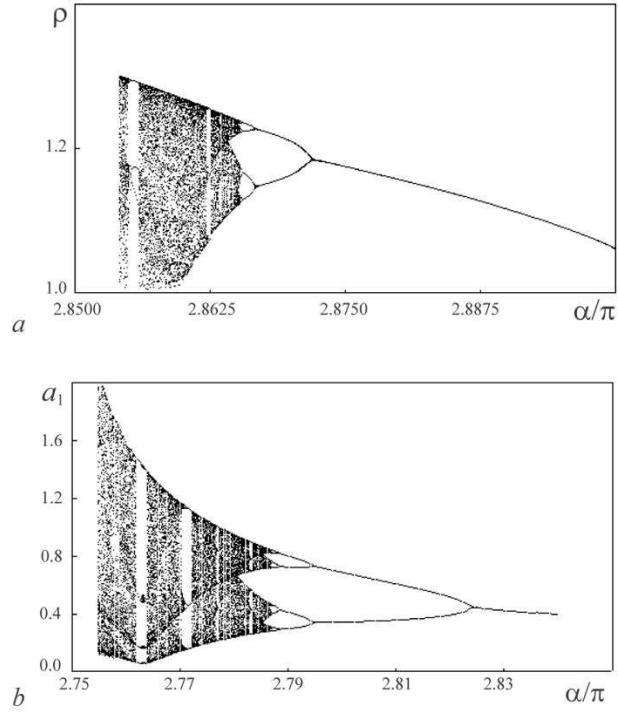


Figure 5: Bifurcation diagrams for the distributed model (a) and the finite-dimensional model (b)

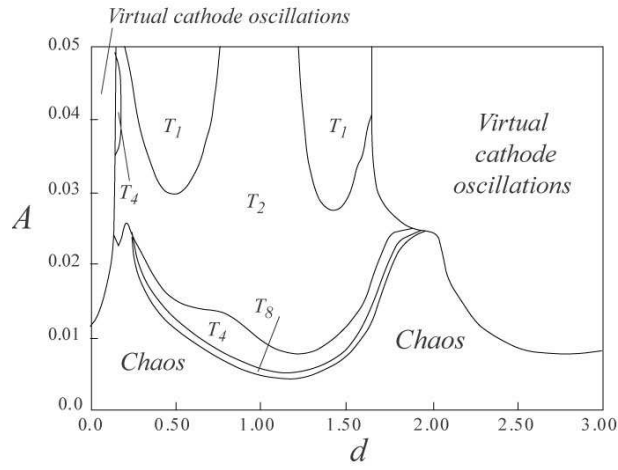


Figure 6:  $A$ - $d$  parameter plane for the finite-dimensional model with delay feedback,  $\alpha = 2.86\pi$

one can see that the finite-dimensional model gives a very good description of the processes taking place in the distributed system.

## 5 Conclusion

In our work the delay feedback influence on the electron beam dynamics in hydrodynamical and finite-dimensional models of Pierce diode is investigated. It is shown that with some feedback parameters' values the chaotic dynamics of the electron beam is suppressed and periodical regimes of different types may be installed. Physically it is connected with the changing of conditions of electron waves propagation. The practical interest for this phenomenon is caused by the ability of eliminating the undesirable parasitical and chaotical oscillations in some real systems where Pierce instability may appear (for example, in electron guns, beams of charged particles, etc.).

## Acknowledgements

We are thankful to Corresponding Member of Russian Academy of Sciences, Prof. D.I. Trubetskov for the fruitful discussion of our work.

The work is supported by Russian Basic Research Fund (grant No 02–02–16351) and grant REC–006 of U.S. Civilian Research & Development Foundation for the Independent States of the Former Soviet Union (CRDF)).

## References

- [1] Pierce J. Limiting currents in electron beams in presence of ions. *J.Appl.Phys.*, **15**, 721 (1944).
- [2] Trubetskov D.I., Hramov A.E. Lectures on microwave electronics for physisists. Vol. 1. Moscow, Nayka, Fizmatlit, 2003 (In Russian).
- [3] High Power Microwave Sources / Ed. by Granatstein V.L. and Alexeff I., Boston, Artech Hourse, 1987.

- [4] Crystal T.L., Kuhn S. Particle simulations of the low  $\alpha$  Pierce diode. *Phys.Fluids*, **28**, 2116 (1985).
- [5] Kuhn S., Ender A. Oscillatory nonlinear flow and coherent structures in Pierce-type diodes. *J.Appl.Phys.* **68**, 732 (1990).
- [6] Anfinogentov V.G., Trubetskov D.I. Chaotic oscillations in the hydrodynamical model of Pierce diode. *Journal of communication technology and electronics*, **38**, 106 (1993).
- [7] Lindsay P.A., Chen X. Xu H. Plasma electromagnetic field interaction and chaos. *International Journal of Electronics*, **79**, 237 (1995).
- [8] Kolinsky H., Schamel H. Counter streaming electrons @ ions in Pierce like diodes. *Phys.Rev.E*, **52**, 4267 (1995).
- [9] Matsumoto H., Yokoyama H., Summers D. Computer simulation of the chaotic dynamics of the Pierce beam-plasma system. *Phys.Plasmas*. **1**, 177 (1996).
- [10] Ott E., Grebogi C., Yorke J.A. Controlling chaos. *Phys. Rev. Lett.* **64**,11 (1990) 1196.
- [11] Pyragas K. *Phys. Lett. A***181** (1992) 203
- [12] Chen Y.H., Chou M.Y. *Phys. Rev. E*. **50**,3 2331 (1994).
- [13] Kaart S., Schouten J.C., van der Bleek C.M. Synchronizing chaos in an experimental chaotic pendulum using methods from linear control theory. *Phys. Rev. E*. **59**,5 5303 (1999).
- [14] Kouomou Y.C., Woafu P. Stability and optimal parameters for continuous feedback chaos control. *Phys. Rev. E*. **66** 036205 (2002).
- [15] Boccaletti S., Bragard J., Arecchi F.T. Controlling and synchronizing space time chaos. *Phys. Rev. E*. **59**,6 6574 (1999).



- [16] Hramov A.E. Effect of feedback on oscillation characteristics of a device with virtual cathode. *Journal of Communication Technology and Electronics*, **44**, 111 (1999).
- [17] Friedel H., Grauer R., Spatschek H.K., Controlling chaotic states of a Pierce diode, *Physics of Plasmas* **5** (1998), No. 9, 3187–3194.
- [18] Krahnstover N. et al, Controlling Chaos in the Pierce Diode. *Phys. Lett. A* **239** 103 (1998).
- [19] Koronovskii A.A., Rempen I.S., Hramov A.E. Controlling chaos in electron beam with overcritical current in fluid model of diode Pierce. *Tech. Phys. Lett.* **29**, 12 (2003).
- [20] Kueny C.S., Morrison P.J. Nonlinear instability and chaos in plasma wave-wave interaction. *Physics of Plasmas*, **2**, 1926 (1995).
- [21] Roache P.J. *Computation fluid dynamics*. Hermosa, Albuquerque, NM, 1972.
- [22] Grassberger P., Procaccia J. On the characterization of strange attractors. *Phys.Rev.Lett.* **5**, 364 (1983).
- [23] Wolf A., Swift J., Swinney H.L., Vastano J. Determining Lyapunov exponents from a time series. *Physica D.* **16**, 285 (1989).
- [24] Takens F. Detecting strange attractors in dynamical systems and turbulence. Lectures Notes in Mathematics, Warwick 1980 / Eds Rand D. and Young L.–S. N.Y.: Springer–Verlag. 1981. P. 366.
- [25] Yagata H. *Progr. of Theor. Phys.*, **78**, 282 (1987).
- [26] Godfrey B.B. Oscillatory non-linear electron flow in Pierce diode. *Phys. Fluids*, **5**, 1553 (1987).